

# Photoluminescence studies of individual and few GaSb/GaAs quantum rings

Cite as: AIP Advances 4, 117127 (2014); <https://doi.org/10.1063/1.4902177>

Submitted: 12 September 2014 . Accepted: 07 November 2014 . Published Online: 17 November 2014

M. P. Young, C. S. Woodhead, J. Roberts, Y. J. Noori, M. T. Noble, A. Krier, E. P. Smakman,  P. M. Koenraad,  M. Hayne, and R. J. Young

## COLLECTIONS

Paper published as part of the special topic on [Chemical Physics](#), [Energy, Fluids and Plasmas](#), [Materials Science](#) and [Mathematical Physics](#)



View Online



Export Citation



CrossMark

## ARTICLES YOU MAY BE INTERESTED IN

[GaSb quantum rings in GaAs/Al<sub>x</sub>Ga<sub>1-x</sub>As quantum wells](#)

Journal of Applied Physics **119**, 044305 (2016); <https://doi.org/10.1063/1.4940880>

[Blueshifts of the emission energy in type-II quantum dot and quantum ring nanostructures](#)

Journal of Applied Physics **114**, 073519 (2013); <https://doi.org/10.1063/1.4818834>

[Excitation power dependence of photoluminescence spectra of GaSb type-II quantum dots in GaAs grown by droplet epitaxy](#)

AIP Advances **6**, 045312 (2016); <https://doi.org/10.1063/1.4947464>



Call For Papers!

## AIP Advances

# SPECIAL TOPIC: Advances in Low Dimensional and 2D Materials

## Photoluminescence studies of individual and few GaSb/GaAs quantum rings

M. P. Young,<sup>1</sup> C. S. Woodhead,<sup>1</sup> J. Roberts,<sup>1</sup> Y. J. Noori,<sup>1</sup> M. T. Noble,<sup>1</sup>  
 A. Krier,<sup>1</sup> E. P. Smakman,<sup>2</sup> P. M. Koenraad,<sup>2</sup> M. Hayne,<sup>1</sup> and R. J. Young<sup>1,a</sup>

<sup>1</sup>*Department of Physics, Lancaster University, LA1 4YB, United Kingdom*

<sup>2</sup>*Department of Applied Physics, Eindhoven University of Technology, The Netherlands*

(Received 12 September 2014; accepted 7 November 2014; published online 17 November 2014)

We present optical studies of individual and few GaSb quantum rings embedded in a GaAs matrix. Contrary to expectation for type-II confinement, we measure rich spectra containing sharp lines. These lines originate from excitonic recombination and are observed to have resolution-limited full-width at half maximum of 200  $\mu\text{eV}$ . The detail provided by these measurements allows the characteristic type-II blueshift, observed with increasing excitation power, to be studied at the level of individual nanostructures. These findings are in agreement with hole-charging being the origin of the observed blueshift. © 2014 Author(s). All article content, except where otherwise noted, is licensed under a Creative Commons Attribution 3.0 Unported License. [<http://dx.doi.org/10.1063/1.4902177>]

Semiconductor nanostructures are appealing for applications in both classical<sup>1</sup> and quantum optoelectronics.<sup>2</sup> Devices containing them promise a wide array of benefits over traditional structures, ranging from increased efficiency with reduced running costs<sup>3</sup> to providing access to useful new phenomena.<sup>4</sup> Nanostructures of GaSb embedded in GaAs are being actively studied as this material system offers access to an unusual combination of physical attributes with some desirable properties. The system can have a type-II band alignment<sup>5</sup> with heavy-holes strongly quantum confined well above room temperature,<sup>6</sup> whilst electrons are confined in the surrounding material via the Coulomb interaction. This asymmetric confinement for the two carrier types could offer advantages in applications such as solar cells,<sup>7</sup> in which reduced exciton binding is beneficial. For light generation purposes, however, the reduction in electron-hole overlap could be detrimental to operating performance. Fabrication of GaSb/GaAs nanostructures by molecular beam epitaxy (MBE) has been shown to result in the formation of nano-rings,<sup>8–10</sup> rather than dots, under specific growth conditions. GaSb quantum rings [Fig. 1(a)] have recently been studied in bulk optical measurements,<sup>9–12</sup> and found to have some surprising optical properties. Cross-sectional scanning tunnelling microscopy (x-STM) has revealed that the ring geometry can confine the electron's wavefunction in its centre,<sup>13</sup> as illustrated in the band diagram in Fig. 1(b). This spatial confinement of the electron may be responsible for the strong optical properties measured in the system. This recent work has paved the way for optoelectronic devices containing GaSb/GaAs quantum rings that are fibre-compatible, and operate above room temperature. In this letter we investigate optical emission from individual and few strongly-confining quantum rings in this material system.

The sample in this study was grown by MBE. Three different types of self-assembled GaSb nanostructures form via the Stranski-Krastanov mode of growth: quantum rings, impure clusters and pyramidal quantum dots. A procedure to yield a high proportion of quantum rings has been developed, with the growth details required to achieve this having been reported previously.<sup>14</sup> Fig. 1 illustrates the expected topology and band structure of the quantum rings studied here, with a deep potential well in the valence band confining heavy holes to GaSb rich regions, and geometric confinement of the electrons in the centre of the rings. The large effective mass of the heavy hole,

<sup>a</sup>Corresponding author, email: [aip@r-j-y.com](mailto:aip@r-j-y.com)

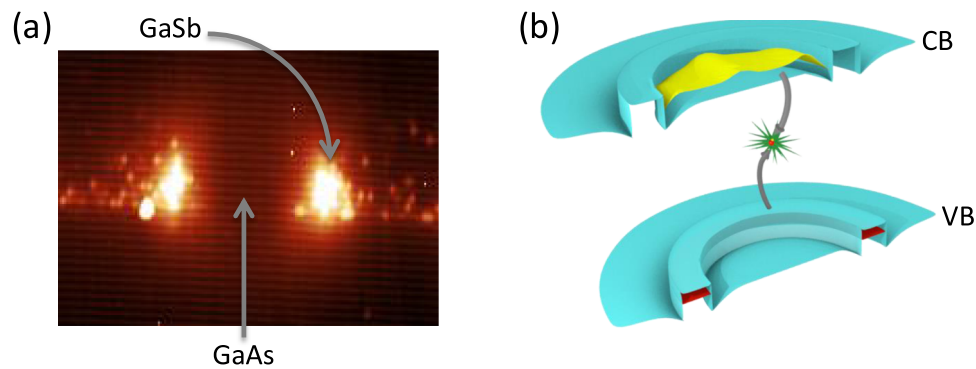


FIG. 1. (a) A cross-sectional scanning-tunnelling image of a GaSb/GaAs ring revealing GaSb lobes; the nanostructures are found to have an average diameter of  $15 \pm 5$  nm.<sup>14</sup> (b) A sketch of the type-II band structure of quantum rings, heavy holes (red) are strongly confined in the valence band (VB) of the GaSb-rich ring, whilst the electron (yellow) is bound by the Coulomb interaction in the conduction band (CB) of the GaAs, and spatially confined to the ring's centre. Photon emission through exciton radiative recombination is illustrated.

and composition modulation in the GaSb nanostructure will likely result in a hole wavefunction that is tightly confined to a small region within the ring structure, rather than occupying the whole circumference. Cross-sectional scanning tunnelling microscopy has helped to reveal the formation mechanism of these nanostructures,<sup>8,14</sup> an example cross-sectional image of a quantum ring is shown in Fig. 1(a). In this image high-antimony-content regions are brighter, compared to those that are arsenic-rich. The two lobes of the ring are clearly visible, and the contrast between the two materials is close to maximal. The density of nanostructures that results from MBE growth can be estimated using cross-sectional measurements and is found to be similar to uncapped samples, in which the density can be directly measured with an atomic force microscope.<sup>15</sup> With the growth parameters used here the quantum ring density in the sample studied is approximately  $1 \times 10^{10} \text{ cm}^{-2}$ .

To enable this study, which required a small number of rings to be isolated, a shadow mask was first added to its surface, followed by a super solid immersion lens (s-SIL).<sup>16</sup> The Ti:Au shadow mask was approximately 100 nm thick, containing 1  $\mu\text{m}$  diameter circular openings, thus allowing groups of  $\approx 100$  rings to be located and relocated using a 50x near-infrared microscope objective. In order to improve our photoluminescence (PL) collection efficiency, an s-SIL with a diameter of 1 mm and a refractive index of 1.8 was bonded to the sample's surface using an index-matched UV-curing epoxy. This lens reduced the spot-size of a continuous-wave excitation laser with a wavelength of 532 nm to  $< 0.25 \mu\text{m}^2$ . The use of a shadow mask under the s-SIL allowed for active position correction of the laser spot during acquisitions, to correct for drift, either manually or using software to drive an XYZ positioning stage. Using this arrangement the number of rings simultaneously excited was reduced to  $\approx 25$ . The significant inhomogeneous broadening present in the dot ensemble, a typical feature of self-organised quantum dots,<sup>17</sup> then enabled emission from individual and few quantum dots to be isolated using spectral filtering. Photoluminescence was collected using the same objective lens used for excitation, with the sample mounted in a cryogen-free cryostat and cooled to 20 K. The emission was analysed by a single-stage spectrometer coupled to an InGaAs diode array.

Fig. 2 shows a typical high-resolution micro-PL ( $\mu\text{PL}$ ) spectrum from the quantum rings at low excitation power (12  $\mu\text{W}$ ). Sharp features in the spectrum are resolution-limited by vibrations from the cryostat, with a full-width at half maximum (FWHM) of  $200 \pm 20 \mu\text{eV}$ , extracted using a Lorentzian fit. The small number of peaks in this spectral range indicates that the spectrum is composed of emission from a few rings. To investigate the optical properties of individual excitonic states confined within the rings, photoluminescence was measured as a function of laser power ranging over three orders of magnitude. The evolution of the emission as a function of laser power for a typical area is shown in Fig. 3.

The emission from type-II confining nanostructures exhibits a characteristic blueshift with increasing excitation power, an effect attributed to asymmetric charging<sup>18</sup> and band-bending.<sup>19</sup> The

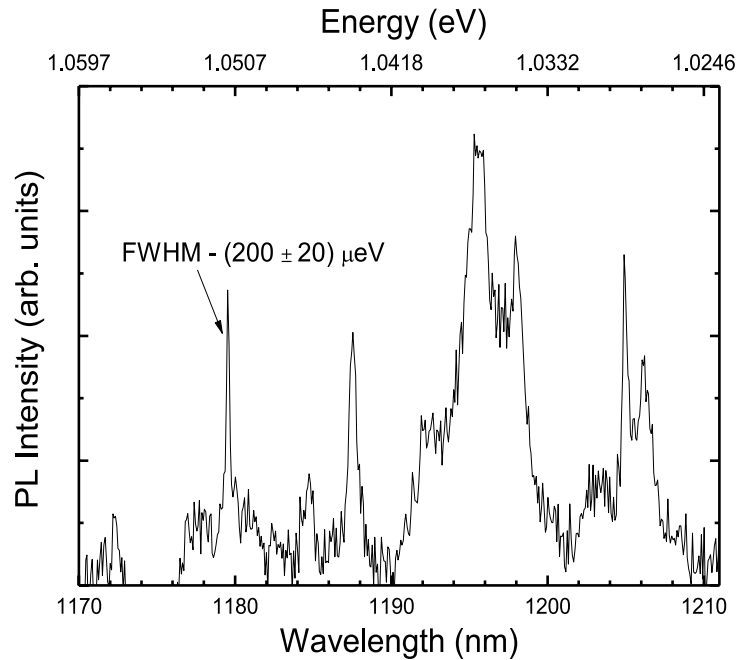


FIG. 2. Micro-photoluminescence from GaSb quantum rings taken at low excitation power. The resolution-limited linewidth of a selected peak is shown.

type-II blueshift was quantified in the fine structure of the rings' emission using two techniques: (i) applying a Lorentzian fit to individual exciton peaks and extracting the central position, and (ii) following a centre-of-mass (CoM) fitting procedure by integrating each  $\mu$ PL spectrum and calculating the point corresponding to the pixel value in which the half-area falls. The results of these two techniques are illustrated at top of the experimental data shown in Fig. 3, and are plotted explicitly in Fig. 4(a). Whilst the positions of individual excitonic lines remain roughly at constant energy with excitation power, the centre-of-mass fit shows a significant and strong blueshift. The latter is witnessed directly in the spectra shown in Fig. 3. As the excitation power is increased, new exciton emission lines tend to appear at shorter (higher) wavelengths (energies); whereas at high excitation power a broad emission background dominates, which noticeably blueshifts. Similar results were measured for a large number of different locations on this sample.

To investigate whether the origin of the blueshift measured in the fine-structure of the exciton spectrum is the same as that of the ensemble, macro photoluminescence was also measured as a function of laser power. A piece of the same wafer, without the shadow mask and SIL, was immersed in liquid helium. Laser light was delivered to the sample via an optical fibre, resulting in an area of  $\sim 2 \text{ mm}^2$  being excited. A second fibre collected the emitted light for analysis. The broad emission spectrum taken from a large ensemble of dots was measured over a large range of excitation powers, and its central position was extracted using a Gaussian peak fitting. The results of these measurements are shown alongside the centre-of-mass fitting from the  $\mu$ PL measurements, in Fig. 4(b). To determine the energy shift of the PL centre position ( $E-E_0$ ), a value of  $E_0$ , the emission energy at zero excitation power, was linearly extrapolated from a plot of the CoM PL positions against integrated peak intensity for the low intensity peaks. The calculated energy shifts were plotted against the integrated intensity of the signal, which is found to be proportional to the excitation power in the measurement range and can be measured more accurately. Utilising a log-log scale on this graph, the exponent governing the blueshift can be extracted, by means of a linear fitting. For the  $\mu$ PL the exponent was found to be  $(0.38 \pm 0.04)$  compared to a value of  $(0.44 \pm 0.03)$  for the macro-PL. Other  $\mu$ PL data fitted were found to have similar values to the one given.

The results in Fig. 4(b) show a clear correlation between the blueshift measured in the bulk PL and that seen in the centre-of-mass of the  $\mu$ PL, i.e. the exponents extracted from the log-log

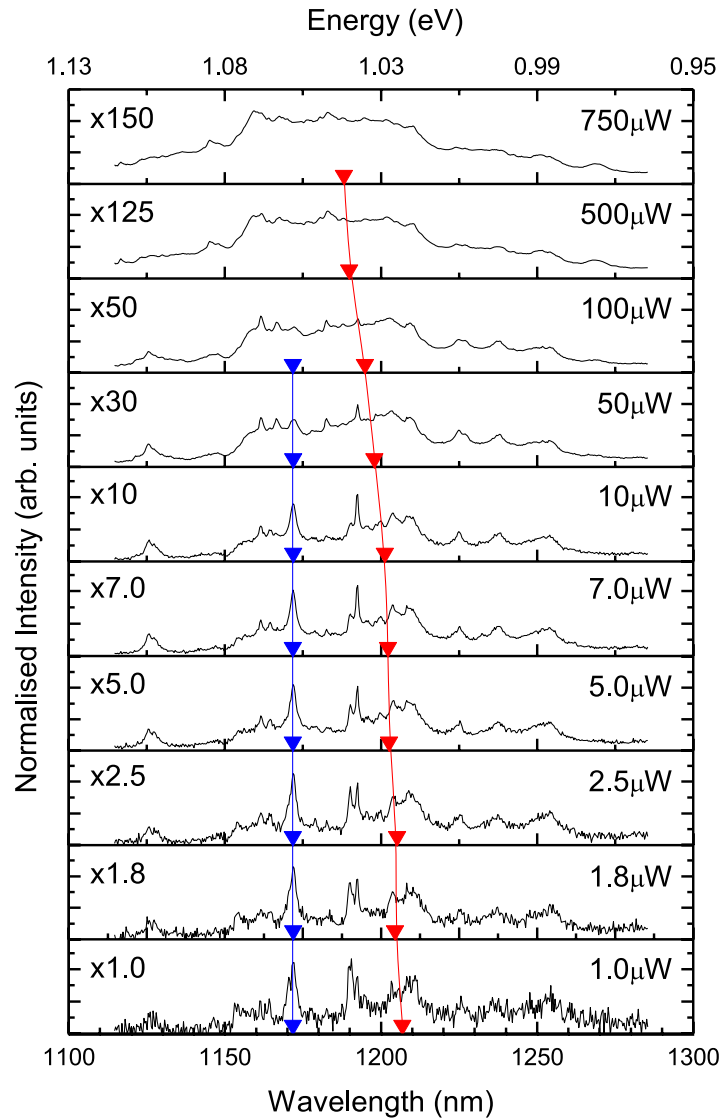


FIG. 3. Micro-photoluminescence from GaSb quantum rings as a function of laser power. Each spectrum was normalised to make the maximum intensity in the spectrum equal. The factors on the left indicate the intensity prior to normalisation, relative to the lowest power spectrum. The blue line tracks the position, extracted using a Lorentzian line fit, of the exciton peak highlighted by the blue arrows, and the red line indicates the position of the centre-of-mass for the entire spectrum.

plot agree within their uncertainties. The two lines do not overlap, but this is expected as the collection efficiencies of the two PL methods used differ, and  $\mu$ PL samples a reduced spectral range. In contrast to this, data for single exciton features show no correlation to the macro PL data. From these measurements we can make a number of conclusions.

The similarity between the blueshifts in the centre-of-mass and macro-PL fittings indicates that the mechanism responsible is constant over a vast range of excitation powers, in contrast to results from Jo *et al.*<sup>20</sup> The power densities for the bulk measurements range from 0.033 to 15  $\text{Wcm}^{-2}$  whilst the  $\mu$ PL power densities range between 3.6 and 2700  $\text{Wcm}^{-2}$ ; combined this suggests a consistent mechanism over five orders of magnitude.

The negligible power-induced shift in the single exciton features is clear evidence that band-bending does not make a significant contribution to the observed blueshift in these nanostructures. If the increasing power density resulted in a bending of the bands, then the energy levels of all confined excitonic states should shift, and this is not observed. As the excitation power increases,

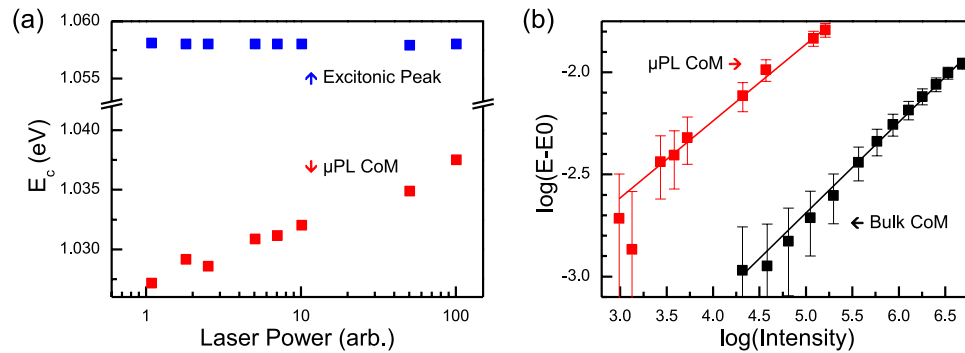


FIG. 4. (a) The position of the exciton emission line and centre-of-mass highlighted in Fig. 3 as a function of excitation power. (b) The corrected centre-of-mass position ( $E-E_0$ ) of the micro- (macro-) photoluminescence spectrum shown in red (black) as a function of integrated intensity.

however, new exciton states appear in the emission spectra, presumably a consequence of the formation of states that are increasingly positively charged. The Coulomb interaction deriving from the asymmetric charging results in an increase in the emission energy as the degree of positive charging increases, which in turn is responsible for the observed blueshift.<sup>21</sup> At high excitation powers the  $\mu$ PL spectra are dominated by broad background features, which may be the result of holes recombining with electrons that are not spatially confined, and/or the number of rings contributing to the spectra may simply be increasing.

In conclusion, we have measured photoluminescence from single GaSb/GaAs quantum rings, which contains surprisingly narrow features at low excitation powers. Sharp features have previously been reported in a more weakly bound hole-confining system,<sup>22</sup> and in an electron confining system,<sup>23</sup> but the quantum rings studied here bind holes very strongly and show promise for fibre-compatible optoelectronic applications. By investigation of the power dependence of the fine structure of the emission from quantum rings it can be concluded that the characteristic blueshift cannot be attributed to band-bending at the heterojunction. The shift appears to arise from the asymmetric filling of higher energy states. These nanostructures may be useful for a wide range of applications and understanding the physics underlying their behaviour is crucial.

This work was supported by the Royal Society through a University Research Fellowship held by R.J.Y.

- <sup>1</sup> D. Bimberg, N. Kirstaedter, N. N. Ledentsov, Z. I. Alferov, P. S. Kopev, and V. M. Ustinov, *IEEE J. Sel. Top. Quantum Electron.* **3**, 196 (1997).
- <sup>2</sup> A. J. Shields, *Nature Photonics* **1**, 215–223 (2007).
- <sup>3</sup> M. Sugawara, N. Hatori, M. Ishida, H. Ebe, Y. Arakawa, T. Akiyama, K. Otsubo, T. Yamamoto, and Y. Nakata, *J. of Phys. D* **38**, 2126 (2005).
- <sup>4</sup> O. Benson, C. Santori, M. Pelton, and Y. Yamamoto, *Phys. Rev. Lett.* **84**(11), 2513–2516 (2000).
- <sup>5</sup> F. Hatami et al., *Appl. Phys. Lett.* **67**, 656 (1995).
- <sup>6</sup> A. Marent, M. Geller, A. Schliwa, D. Feise, K. Pötschke, D. Bimberg, N. Akçay, and N. Öncan, *Appl. Phys. Lett.* **91**, 242109 (2007).
- <sup>7</sup> R. B. Laghumavarapu, A. Moscho, A. Khoshakhlagh, M. El-Emawy, L. F. Lester, and D. L. Huffaker, *Appl. Phys. Lett.* **90**, 173125 (2007).
- <sup>8</sup> R. Timm, H. Eisele, A. Lenz, L. Ivanova, G. Balakrishnan, D. L. Huffaker, and M. Dähne, *Phys. Rev. Lett.* **101**, 256101 (2008).
- <sup>9</sup> R. Timm, H. Eisele, A. Lenz, L. Ivanova, V. Vossebürger, T. Warming, D. Bimberg, I. Farrer, D. A. Ritchie, and M. Dähne, *Nano. Lett.* **10**(10), 3972–3977 (2010).
- <sup>10</sup> P. Carrington, R. J. Young, P. Hodgson, A. M. Sanchez, M. Hayne, and A. Krier, *Cryst. Growth Des.* **13**, 1226 (2013).
- <sup>11</sup> K. Suzuki, R. A. Hogg, and Y. Arakawa, *J. Appl. Phys.* **85**, 8349 (1999).
- <sup>12</sup> I. Farrer, M. J. Murphy, D. A. Ritchie, and A. J. Shields, *J. Crystal Growth* **251**, 771–776 (2003).
- <sup>13</sup> R. J. Young, E. P. Smakman, A. M. Sanchez, P. D. Hodgson, P. M. Koenraad, and M. Hayne, *Appl. Phys. Lett.* **100**, 082104 (2012).
- <sup>14</sup> E. P. Smakman, J. K. Garleff, R. J. Young, M. Hayne, P. Rambabu, and P. M. Koenraad, *Appl. Phys. Lett.* **100**, 142116 (2012).
- <sup>15</sup> A. J. Martin et al., *Appl. Phys. Lett.* **102**, 113103 (2013).
- <sup>16</sup> M. Yoshita, T. Sasaki, M. Baba, and H. Akiyama, *Appl. Phys. Lett.* **73**, 635 (1998).

- <sup>17</sup> W.-H. Lin, M.-Y. Lin, S.-Y. Wu, and S.-Y. Lin, [IEEE Photon. Tech. Lett.](#) **24**, 1203 (2012).
- <sup>18</sup> L. Müller-Kirsch, R. Heitz, A. Schliwa, O. Stier, D. Bimberg, H. Kirmse, and W. Neumann, [Appl. Phys. Lett.](#) **78**, 1418 (2001).
- <sup>19</sup> C.-K. Sun, G. Wang, J. E. Bowers, B. Brar, H.-R. Blank, H. Kroemer, and M. H. Pilkuhn, [Appl. Phys. Lett.](#) **68**, 1543 (1996).
- <sup>20</sup> M. Jo, M. Sato, S. Miyamura, H. Sasakura, H. Kumano, and I. Suemune, [Nanoscale Research Letters](#) **7**, 354 (2012).
- <sup>21</sup> P. D. Hodgson, R. J. Young, M. Ahmad Kamarudin, P. J. Carrington, A. Krier, Q. D. Zhuang, E. P. Smakman, P. M. Koenraad, and M. Hayne, [J. Appl. Phys.](#) **114**, 073519 (2013).
- <sup>22</sup> K. Matsuda, S. V. Nair, H. E. Ruda, Y. Sugimoto, T. Saiki, and K. Yamaguchi, [Appl. Phys. Lett.](#) **90**, 013101 (2007).
- <sup>23</sup> M. P. F. de Godoy et al., [Phys. Rev. B](#) **73**, 033309 (2006).